Proceedings of CONF-MCEE 2026 Symposium: Geomaterials and Environmental Engineering
DOI: 10.54254/2755-2721/2026.MH30690

Simulation-Based Evaluation of EV Charging Configurations and Carbon Reduction Potential in a University Commuter System

Yansong He

School of Civil & Environmental Engineering, Oklahoma State University, Stillwater, USA
yansong.he@okstate.edu

Abstract. This paper examines the performance and potential of CO2 reduction of different configurations of electric vehicle charging infrastructure within a university commuter model, incorporating a simulated population and a discrete event simulation model. A commuter population dataset is created from ZIP code-based population assignment, distance-band approach, and personalized driving pattern models. Various charging infrastructure setups involving level 2 charging and level 3 charging were simulated for 30-day periods, with performance metrics such as wait-time, peak demand, use factor, and infrastructure cost appropriately evaluated. It is seen that performance characteristics significantly enhance beyond a base infrastructure level of 4–5 level 2 charging stations, with wait times diminishing close to zero levels for most level 3 charging setups. A WCDM decision makers' strategy shows the charging setups of (L2=5, L3=0), and (L2=6, L3=0) charging setups being most cost-effective charging options with charging setups involving one level 3 charging station being viable options with excellent performance matrices. Results from CO2 emission calculations reveal net emission a decent reduction potential every month with an eventual shift from internal-combustion engine vehicles to electric vehicles among the simulated commuter population dataset pool.

Keywords: electric vehicle charging infrastructure, discrete-event simulation, multi-criteria decision making, carbon emission reduction, university commuter system

1. Introduction

Air pollution has become a continuously pressing issue that poses serious threats to human health at an astonishing scale, 99% of the world's population was living in places where the WHO air quality guidelines levels were not met in 2019 [1]. Air pollution includes particulate matters (PM), nitrogen oxides (NOx), Volatile Organic Compounds (VOCs), and sulfur dioxide (SO2). Carbon emissions are also counted as a significant part of the air pollution, encompassing carbon dioxide (CO2) and carbon monoxide (CO), which are both critical contributing factors to climate change and potential human health risks [2]. The rise in carbon emissions, mainly caused by human activities, saw an exponential rise since the beginning of the Industrial Revolution around the late 18th to early 19th

DOI: 10.54254/2755-2721/2026.MH30690

century, with most of the increase resulted from increased fossil fuel consumption and industrial emissions [3].

The transportation sector is a major contributor to air pollution and climate change. At the global level, the transportation sector accounts for 20% of the total CO2 emissions with almost 8 Gt metric tons of CO2 was released by the end of 2022 [4]. Notably, “the highest increase in GHG emissions has been realized by the transportation sector in recent decades,” and existing climate policies “have failed to reduce the growth rate of emissions” [5]. These conclusions highlight that the rise in greenhouse gases in the world in the past decades represents a rather important issue, because, in the transportation sector, mitigation actions still appear rather difficult.

2. Literature review

As the problems arising from the continue growing carbon emissions of the transportation sector become more severe, the proposal of electrification of the transportation sector is implemented by the government to help mitigate the issues around various fields such as public health, air quality, and climate change. For instance, electrification of heavy-duty trucks in urban centers like the Greater Toronto and Hamilton Area is projected to reduce GHGs by 10.5% and prevent up to about 200 premature deaths annually due to fine particulates, with the related health co-benefits being mainly concentrated in social disadvantaged neighborhoods [6]. Furthermore, modeling for China indicates that a widespread adoption of heavy-duty EVs could avoid more than 500 premature deaths due to acute poisoning during extreme air pollution events, further underlining the interconnection between potentially improving public health crises together with air quality degradation [7].

Although the complete adoption of electrification in the transportation sector isn’t viable due to several challenges such as the infrastructure demands and the high upfront costs, it can still pave the roads for the sustainable urban transportation even at a smaller scale. Recent modeling work confirms this perspective. For example, optimization work using the genetic algorithm approach on the charging infrastructure in the city has revealed that a properly organized charging network can adequately service the needs of the bulk of the city's electric-vehicle users. In a real-world case study for Thessaloniki, the model demonstrated that “15 stations would be required to cover 80% of the estimated electric vehicles charging demand” [8]. The results have made it clear that properly organized access to charging points in the major zones of activity can improve range anxiety and encourage the adoption process even in an immature infrastructure environment.

Based on the preceding work, the proposed study seeks to contribute to the discussion on the role that optimization methods can play in the planning and implementation process related to the transportation sector and the issue of its decarbonization. In the scientific field, there are sufficient studies on the problem and the opportunities offered using electric-vehicle technology in an urban setting. However, there still exists a gap in terms of tools that can help in the implementation process.

DOI: 10.54254/2755-2721/2026.MH30690

3. Methodology

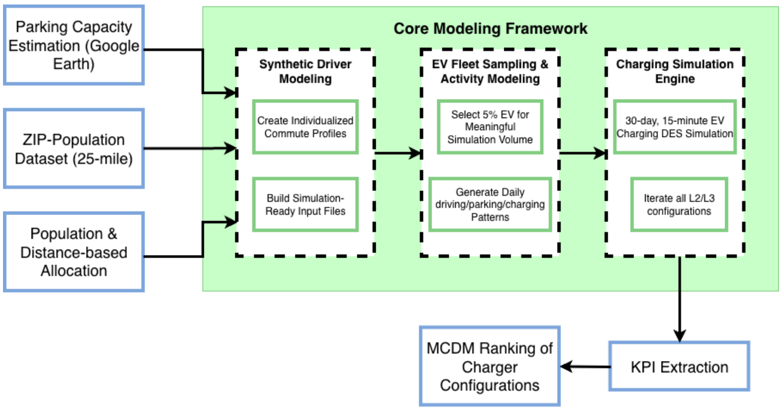

Figure 1. A scheme flow diagram

3.1. Parking capacity estimation

The overall workflow of the modeling process is illustrated in Figure 1, which summarizes the major steps from parking capacity estimation to KPI extraction. The number of parking spaces was estimated utilizing Google Earth satellite imagery of the parking lot, since there was no sufficient information regarding the number of parking spaces from the university officials. The boundaries of the parking lot were marked manually, and the number of parking spaces were estimated using the standard dimensions of a US parking space. This scheme offers a reasonable approximation of the number of commuters the charging system is expected to serve.

3.2. ZIP-code population dataset

The data on the demographic information of the ZIP codes was derived from UnitedStatesZipCodes.org and selected to only contain the locations of the centroid of the ZIP code within a 25-mile radius of the location of the study. The haversine formula was used to find the distance from each centroid of the ZIP code to the parking lot. This data set defines the possible geographic points of origin of everyday commuters.

3.3. Population & distance-based allocation

The commuters are distributed to the zip codes based on a weighted allocation method that utilizes the size of the population and pre-defined distance bands (0-10 miles and 10-25 miles). This method will guarantee the novel commuter cohort simulates the local population density and the possible commute patterns. This allocation will be used as the building blocks for constructing the commuter profiles.

3.4. Synthetic driver modeling

Individualized syntheses of the driver profiles were created, which considered home geolocation information, commute distance, commute duration, and arrive/departure schedules. Random elements were introduced to represent variations of real-world commute behaviors. This data is the crucial input used in modeling of the EV activity.

DOI: 10.54254/2755-2721/2026.MH30690

3.5. Simulation-ready input file construction

All the synthetically derived driver profiles were converted into the input format required in the EV-Infrastructure-tool and saved as structured json. files. This json. file helps in maintaining compatibility requirements of the simulation engine and helps in standardizing the characteristics of the driver profiles.

3.6. EV fleet sampling

An adoption level of 5% of EVs is considered in this study not to represent the reality of the situation but to provide enough EVs in the system to allow the system to be meaningfully simulated. EV users are randomly selected from the artificial commuter traffic. This step determines the EVs that will interact in the system.

3.7. EV charging simulation

A discrete event simulation (DES) was run over a period of 30 days at a timestep of 15 minutes using the EV-infrastructure-tool. The DES allows the simulation of the interaction dynamics of the EVs and the charge network through the state of charge update of the vehicles and the allocation of EVs to available level two and level three charge points.

3.8. KPI extraction

In each charger-count pair (L2: 1 to 9, and L3: 0 to 2), the simulation was run independently. The basic results of the simulation, which appeared in the file pov_vehicle_status.csv, were then analyzed through the output-analysis.py script provided in the tool to extract the results of the key performance indicators: waiting time, peak demand, utilization rate, and infrastructure costs. Afterwards, the results were then presented through graphical representation of the heat maps and summaries.

3.9. MCDM ranking of charger configurations

A weighted Multi-Criteria Decision Making (MCDM) model has been used to prioritize the charging arrangements regarding the costs, waiting time, utilization rate, and the maximum electrical load. The selected Key Performance Indicators (KPIs) will be normalized and combined based upon the pre-set weights. This will provide the best optimized and cheapest approach in designing the charging infrastructure.

4. Driving model development

4.1. Study area characterization and synthetic driver population modeling

4.1.1. Parking lot capacity estimation

Since no related data that are publicly provided on the actual capacity of the external parking lot at Boone Pickens Stadium, high-resolution satellite images provided by Google Earth were utilized to estimate the parking capacity, as shown in Figure 2. The boundary lines on the parking lot are manually identified, followed by estimates for the number of parking spaces within the lot using stall-width-based estimation. This estimate provides sufficient simulation data for parking capacity

DOI: 10.54254/2755-2721/2026.MH30690

estimation while also ensuring clarity on how estimates are derived. The estimate provided for parking capacity is then utilized for EV adoption simulation.

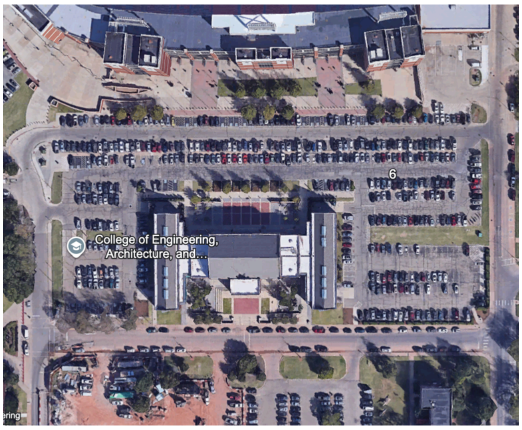

Figure 2. Aerial view of the parking lot

4.1.2. ZIP code-based population characterization

To identify and classify the residential areas for potential parking lot users, ZIP code demographic information was collected from United States Zip Codes.org, an additional population heat map is shown in Figure 3. Geographic center coordinates in terms of latitude and longitude, as well as the population size in every ZIP code, are the information that are showcased and then collected from the website. ZIP codes within 25 miles surrounding the parking lot location are identified to reasonably delimit the commuter range area for Oklahoma State University. This geographic filter provided a group of ZIP codes that together identify the regional population likely to contribute to daily parking demand. This group of ZIP codes provided input to create the synthetic commuter data set.

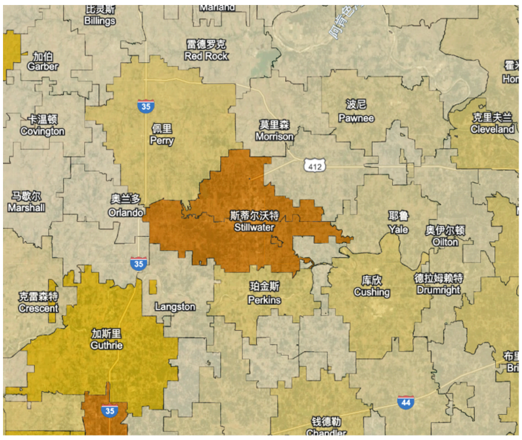

Figure 3. Population heat map

A population heat map from Google Earth illustrates ZIP-code density using a light-to-dark color gradient, where darker orange regions represent higher population concentrations (up to ~28,500 residents).

DOI: 10.54254/2755-2721/2026.MH30690

4.1.3. Synthetic driver generation based on population and distance distribution

To represent real-world travel behavior, a synthetic population of drivers was created using the script generate_employees.py created as an ancillary study to this research. A total of 455 commuting vehicles were allocated to the identified ZIP codes based not only on population but also according to a predefined distance distribution for commuting. To distribute the total number of synthetic drivers in each distance band to specific ZIP codes proportional to their probabilities weighted by population, each distance band had the aggregate number of synthetic drivers allocated to individual ZIP codes. A full commuting profile to be followed by every commuter was created by this simulation. Every driver had their residential type of charging randomly allocated to be either Level 1 or Level 2. The data set from this simulation was then exported to update_employee_commute.json in conformity with EV-Infrastructure Simulation Tool.

4.2. EV charging model

4.2.1. EV user selection and activity pattern construction

Although the synthetic commuter data set represents 455 vehicles ranging from 0-25 miles to the central location, not all of these represent the commuting population labeled for simulation to use electric vehicles. Instead of choosing the adoption rate to be reflective of data from the state, it was decided a fixed 5% would be designated to ensure it captured enough electric vehicles for the experiment to be meaningfully representative in simulation data sets. A low adoption rate would not provide enough data to meaningfully contrast results across configurations. A time-resolved driving and parking activity schedule was created for each of the identified electric vehicle commuters via application of the functions available in package 'ev-infrastructure-tool’. The detailed timelines of all electric vehicles were merged into 'pov_drive_pattern.json’ and were direct inputs to be used in the simulation of charging management

4.2.2. EV charging simulation framework

The simulation of charging processes is conducted using a discrete-events simulation engine embedded in the script standalone-pov-charging-management_short.py. The simulation runs for a 30-day cycle with discrete steps of 15 minutes to allow development of systemic dynamics of electric vehicle charging.

In each time step, it executes these operations:

• Updates electric vehicle (EV) locations and state of charge (SOC),

• Manages the charging queue via the internal framework modules,

• Distributes Level 2 and Level 3 charging stations to vehicles awaiting service.

• Processes active charging sessions by increasing SOC and resets the system state to reflect turnover at real-world boundaries of time.

The capabilities for charging have been modeled using two types of stations: Level 2 charging stations rated 19.2 kW and Level 3 fast stations rated 60 kW. This discrete-event approach captures interactions between EV arrival patterns, queue formation, charging station availability, and electrical load.

DOI: 10.54254/2755-2721/2026.MH30690

4.2.3. Charger configuration iteration and post-processing of performance metrics

To evaluate the effect of different configurations of charging stations, discrete simulation of events was performed for a matrix of stations classified according to Level 3 chargers from 0 to 2 stations and Level 2 chargers from 1 to 9 stations. The simulation for all scenarios had identical electric vehicle activities to ensure fair results, simultaneously, it also maintained time-series data about all activities performed by electric vehicles, such as arrival, queueing, charging, state-of-charge changes, and allocation to stations, in a file specific to each configuration named 'pov_vehicle_status.csv’. After completion of each simulation run, performance indicators were calculated for the system level by using post-processing scripts, named 'output_analysis.py’, which belonged to the "ev-infrastructure-tool." These KPI values were then extracted and visualized manually. Heatmaps, ranking tables, and comparative plots were produced to illustrate the performance across all (L2, L3) configurations. The processed KPI dataset served as the foundation for the multi-criteria optimization stage described in Section 4.2.

5. Results

5.1. Simulation output analysis and visualization

5.1.1. KPI summary table for all charger configurations

The following Table 1 gives a combined overview of the system performance metrics studied across various L2 – L3 charge settings. As expected, the installation costs continue to escalate as the number of charge points increases, while the waiting times reduce in a nonlinear fashion once the minimal infrastructural requirements are met. The maximum demand truly escalated within settings involving L3 charge points because of their larger power ratings, while the usage factors reduced with each additional charge point introduced due to congestion alleviation. The above trends broadly outline the major compromises involved in various system settings regarding financial costs, performance characteristics, and power handling.

Table 1. Key Performance Indicators (KPIs) for different charging-station deployment scenarios

KPIs	L3/L2	1	2	3	4	5	6	7	8	9
Installation cost ($)	0	$20,000	$40,000	$60,000	$80,000	$100,000	$120,000	$140,000	$160,000	$180,000
Installation cost ($)	1	$95,000	$115,000	$135,000	$155,000	$175,000	$195,000	$215,000	$235,000	$255,000
Installation cost ($)	2	$170,000	$190,000	$210,000	$230,000	$250,000	$270,000	$290,000	$310,000	$330,000
Waiting time (hours)	0	1668	495	224	64	0	0	0	0	0

DOI: 10.54254/2755-2721/2026.MH30690

Table 1. (continued)

Waiting time (hours)	1	197	97	32	0	0	0	0	0	0
Waiting time (hours)	2	64	0	0	0	0	0	0	0	0
Peak demand (kW)	0	38.4	76.8	115.2	153.6	192	192	192	192	192
Peak demand (kW)	1	218.4	256.8	295.2	273.6	192	192	192	192	192
Peak demand (kW)	2	398.4	436.8	355.2	273.6	192	192	192	192	192
Utilization rate	0	0.59895833	0.45182292	0.38932292	0.31282552	0.24895833	0.20746528	0.17782738	0.15559896	0.13831019
Utilization rate	1	0.5625	0.38758681	0.32291667	0.25807292	0.20746528	0.17782738	0.15559896	0.13831019	0.12447917
Utilization rate	2	0.40321181	0.31119792	0.25807292	0.21506076	0.17782738	0.15559896	0.13831019	0.12447917	0.11316288

5.1.2. Monthly mileage distribution of the synthetic commuter population

Figure 4 shows the distribution of monthly commute distance of the synthetic commuter population, which indicates a short commute length distribution along with a long tail of longer commute distances corresponding to the higher-mileage commute. This distribution helps in understanding the weighting factor used in the model simulations.

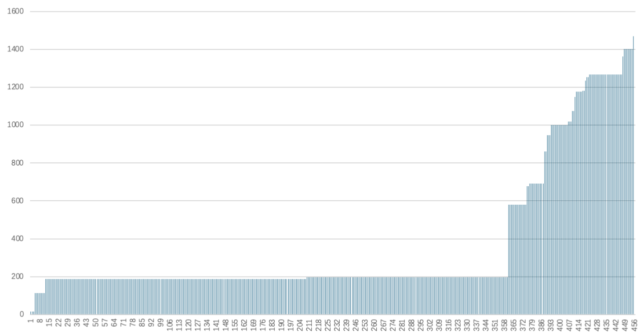

Figure 4. Monthly mileage distribution graph

5.1.3. Waiting time across L2/L3 charger combinations

Figure 5 shows the waiting times of the different configurations considered, which vary from 1 to 9 for the number of L2 charging stations, and from 0 to 2 for the number of L3 charging stations. Those configurations involving only 1–2 stations of type L2 and no stations of type L3 will display the maximum waiting times, showing that the network has inadequate provision. The waiting time reduces considerably when there are 4–5 stations of type L2 installed or at least one station of type L3 has been installed; thereafter, most of the configurations will approach zero waiting time.

DOI: 10.54254/2755-2721/2026.MH30690

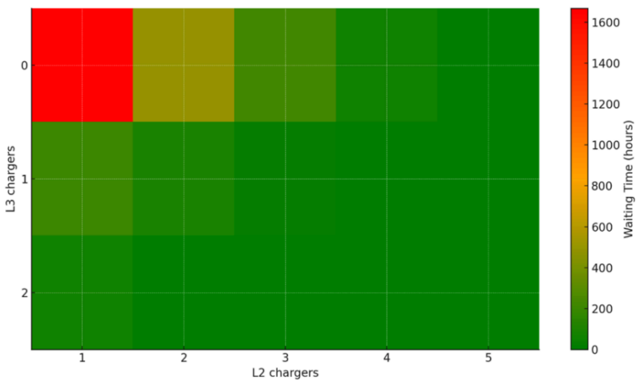

Figure 5. Waiting times heat map

5.1.4. Charger utilization rates under different L2/L3 configurations

Figure 6 presents the usage of the Chargers found in the various setups of L2 and L3 Chargers from 1–9 of the latter and 0–2 of the former. The trend confirms the usage of the Chargers as being maximum in the low-capacity setup involving only one and two L2 Chargers. The addition of more L2 Chargers, especially the introduction of an L3 Charger in the setup, leads to the gradual fall of usage of the Chargers indicating less competition regarding the usage of the Chargers.

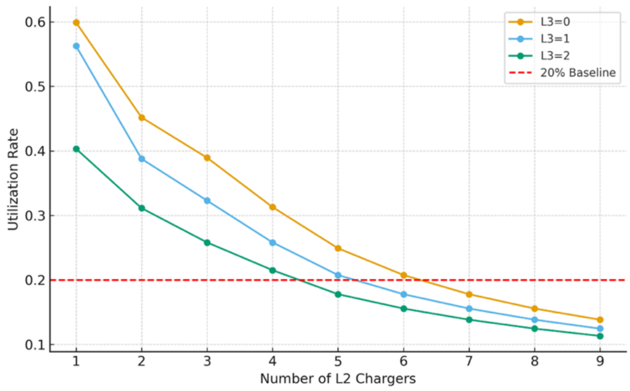

Figure 6. Utilization rate line chart

5.1.5. Peak demand for all charging infrastructure scenarios

In Figure 7, it becomes evident that there's a stabilization of the peak at about the value of 192 kW in almost all possible arrangements. This happens because of the charge logic that favors Level 2 Chargers first until the maximum number of Level 2 units are used at the same time as the maximum number of Level 3 units can be used when there's not enough level 2 charge available. This results in a consistent peak value even when the network arrangement involves level 3 charge units.

DOI: 10.54254/2755-2721/2026.MH30690

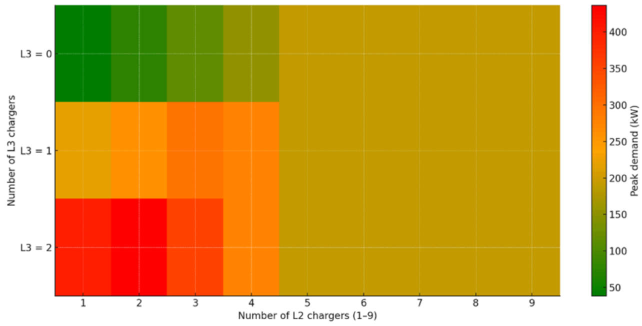

Figure 7. Peak demand heat map

5.2. Multi-Criteria Decision Making (MCDM) optimization

To determine which charger configuration performs the best, a weighted Multi-Criteria Decision Making (MCDM) methodology was used. The following four criteria were considered for evaluation:

- Waiting time (40% weight) – lower is better
- Cost of infrastructure (30% weight) – lower is better
- Utilization rate (20% weight) – deviation from a 20% operational target is penalized
- Peak demand (10% weight) – lower is better

A normalization step involving min/max scaling based on observed ranges across all simulation runs was applied to each metric. The weighted sum of these normalized values resulted in a composite score for each (L2, L3) pair. The calculating steps are as followed:

$w_{time} = 0.40$, $w_{cost} = 0.30$, $w_{util} = 0.20$, $w_{peak} = 0.10$

The assigned weights reflect the relative importance of each criterion, with waiting time prioritized most heavily and peak demand least.

$$N_{cost} = \frac{x_{max} - x}{x_{max} - x_{min}} \tag{1}$$

In Equation (1), x is the cost of the scenario being evaluated, while x_{max} and x_{min} are the highest and lowest costs among all scenarios. N_{cost} is the normalized cost value.

This expression scales infrastructure cost so that lower-cost configurations receive higher normalized scores.

$$N_{peak} = \frac{x_{max} - x}{x_{max} - x_{min}} \tag{2}$$

In Equation (2), x refers to the peak demand of the scenario, and x_{max} and x_{min} are the maximum and minimum peak-demand values observed in the dataset. N_{peak} is the normalized peak-demand value.

Peak demand is normalized in the same manner, rewarding scenarios with lower electrical loading.

$$N_{util} = 1 - \frac{|x - x_{baseline}|}{x_{max} - x_{min}} \tag{3}$$

In Equation (3), x is the utilization value of the scenario, $x_{baseline}$ is the target utilization level, and x_{max} and x_{min} represent the highest and lowest utilization values. N_{util} is the normalized

DOI: 10.54254/2755-2721/2026.MH30690

utilization value.

Utilization is evaluated by penalizing deviations from the 20% operational target, yielding higher scores for values closer to the baseline.

$$N_{wait} = \frac{x_{max} - x}{x_{max} - x_{min}} \quad (4)$$

In Equation (4), x represents the waiting time of the scenario, with x_{max} and x_{min} indicating the longest and shortest waiting times across all scenarios. N_{wait} is the normalized waiting-time value.

Waiting time is normalized to favor configurations that minimize queueing delays.

$$S = 0.4\ N_t + 0.3\ N_c + 0.2\ N_u + 0.1\ N_p \quad (5)$$

In Equation (5), N_t , N_c , N_u , and N_p are the normalized values for waiting time, cost, utilization, and peak demand. S is the final combined score.

The final score is a weighted linear combination of all normalized metrics, producing an overall ranking of charger configurations.

The partial calculated results are shown in Table 2:

Table 2. MCDM results

Ranking	L3	L2	Cost ($)	Wait (h)	Peak (kW)	Utilization	Score
1	0	5	100,000	0	192.0	0.248958	0.864
2	0	6	120,000	0	192.0	0.207465	0.862
3	0	4	80,000	64	153.6	0.312826	0.851
4	0	7	140,000	0	192.0	0.177827	0.836
5	0	3	60,000	224	115.2	0.389323	0.810
6	1	5	175,000	0	192.0	0.207465	0.808
7	0	8	160,000	0	192.0	0.155599	0.808
8	1	4	155,000	0	273.6	0.258073	0.786
9	1	6	195,000	0	192.0	0.177827	0.783
10	0	9	180,000	0	192.0	0.138310	0.781

The results of the MCDM analysis clearly bring out the performance trends of the various L2/L3 charger arrangements. The best-performing "pure" L2 arrangements involving five to six L2 chargers (and consequently an L3 value of 0) obtain the highest combined ratings of at least 0.86, thanks to the least peak demand, no waiting time, and relatively low installation costs. These arrangements are technically sound because they achieve the twin objectives of efficient costs and reliable performance without incorporating the large power of DC fast charging.

Configurations involving single L3 charger (L3 = 1, L2 = 5) provide the best possible trade-off regarding performance of the system and user convenience. This configuration provides quick charging support along with no waiting time and usage close to the targeted level of 20% operation of the system, hence yielding a competitive value (~0.81).

A slightly more conservative but still valid option is the scheme, L3 = 1, L2 = 4, which provides a high level of cost-effectiveness and acceptable usage levels at the price of a slightly increased

DOI: 10.54254/2755-2721/2026.MH30690

system load. The above three options cover different implementation scenarios: from frugal solutions based solely on L2 to optimized heterogeneous network setups.

6. Discussion

The environmental advantage of supplementing the commuter group with electric cars can be determined by comparing the emissions characteristics of internal combustion engine cars and electric cars. The United States Environmental Protection Agency describes the approximate consumption of a gasoline-powered car at 404 g/mile. Electric cars, on the other hand, do not produce direct emissions, and the sole factor contributing to their indirect emissions would be the energy intensity of the source energy used in the charging process [9]. Using an average energy consumption rate in electric cars of 34.6 kWh/100 miles, as provided by GenCell Energy, and the adopted unit emission factor contribution from the energy source, 0.321442 kg CO_2/kWh, from Climatiq, the mileage-wise emission factor would be approximately 0.111 kg/mile [10, 11].

In the synthetic commuter dataset utilized in this work, the sum of the one-way distances driven by the 455 commuters combines to 2,750.9 miles. In a 22-day work month and round-trip driving, the sum of the commuter miles each month would be 121,039.6 miles. Furthermore, the sum of the estimated emissions in the present scenario, where all commuters use ICEVs, would be approximately 48,900 kg/month, and would be lowered considerably when all commuters use EVs, resulting in an average sum of approximately 13,462 kg/month, an indicator that the adoption could potentially lower emissions by 35,438 kg/month. Keeping in mind the assumed mean adoption rate in the present work to be 5%, the resultant reduction would proportionally alter and potentially lower the sum by approximately 1,772 kg/month.

7. Conclusion

The paper evaluates the charging environment on a campus, reflecting the first step in understanding the broader implications related to the transportation transition. In effect, the demand for charging the electric vehicle goes beyond the normal commuting range and considers long-distance travel, corridor charging, public accessibility, and the limitations imposed by the power grid. The complexity and broader implications related to the power transition on a large nation are reflected in the charging scenario models, as outlined in the 2030 National Charging Network, conducted by the National Renewable Energy Laboratory [12].

To contextualize the results obtained in the campus-level scenario, the EVI-X Toolbox figures on a statewide basis indicate that there are approximately 1,435 charging events and 63,130 kWh of energy consumption daily in the State of Oklahoma, figures that far exceed the demands determined in the commuter scenario [13]. The State provides 509 DC fast-charging connections across 115 stations and maintains a 5,714-mile-long highway network. The figures at the statewide level make it clear that fast-charging needs, long-distance travel, and peak loads on the energy network, with a peak of 46 MW, representing important factors that cannot be accounted for in the commuter scenario on a single-campus network. The scenario discussed in this paper therefore needs to be viewed as a micro-level case that may, in the future, be expanded to include factors related to a larger scale.

References

[1] World Health Organization. (2024). Ambient (outdoor) air quality and health. https: //www.who.int/news-room/fact-sheets/detail/ambient-(outdoor)-air-quality-and-health

DOI: 10.54254/2755-2721/2026.MH30690

[2] Hadipoor, M., Keivanimehr, F., Baghban, A., Ganjali, M. R., & Habibzadeh, S. (2021). Carbon dioxide as a main source of air pollution: Prospective and current trends to control. In A. Nunez-Delgado (Ed.), Sorbents materials for controlling environmental pollution: Current state and trends (pp. 623–688). Elsevier. https: //doi.org/10.1016/B978-0-12-820042-1.00004-3
[3] U.S. Environmental Protection Agency. (2024). Global greenhouse gas emissions overview. https: //www.epa.gov/ghgemissions/global-greenhouse-gas-overview
[4] International Energy Agency. (2024). Transport – Energy system. https: //www.iea.org/energy-system/transport
[5] Ülengin, F., Işik, M., Önsel Ekici, Ş., Özaydın, Ö., Kabak, Ö., & Topçu, İ. (2018). Policy developments for the reduction of climate change impacts by the transportation sector. Transport Policy, 61, 36–50. https: //doi.org/10.1016/j.tranpol.2017.09.008
[6] Torbatian, S., Saleh, M., Xu, J., Minet, L., Mahagammulla Gamage, S., Yazgi, D., Yamanouchi, S., Roorda, M. J., & Hatzopoulou, M. (2024). Societal co-benefits of zero-emission vehicles in the freight industry. Environmental Science & Technology, 58(18), 6712–6724. https: //pubs.acs.org/doi/10.1021/acs.est.3c08867
[7] Horton, D. E., Schnell, J. L., Peters, D. R., Wong, D. C., Lu, X., Gao, H., Zhang, H., & Kinney, P. L. (2021). Effect of adoption of electric vehicles on public health and air pollution in China: A modeling study. The Lancet Planetary Health, 5, S8. https: //doi.org/10.1016/S2542-5196(21)00092-9
[8] Efthymiou, D., Chrysostomou, K., Morfoulaki, M., & Aifantopoulou, G. (2017). Electric vehicles charging infrastructure location: A genetic algorithm approach. European Transport Research Review, 9, 27. https: //doi.org/10.1007/s12544-017-0239-7
[9] U.S. Environmental Protection Agency. (2024). Greenhouse gas emissions from a typical passenger vehicle. https: //www.epa.gov/greenvehicles/greenhouse-gas-emissions-typical-passenger-vehicle
[10] Zargary S. (2023). How much electricity does an electric car use? GenCell Energy. https: //www.gencellenergy.com/resources/blog/ev-charging-power-car-electricity-usage/
[11] Climatiq. (2024). Electricity supplied from grid – Emission factor. https: //www.climatiq.io/data/emission-factor/bddedf7c-7897-4690-abf7-564fcb431e7d
[12] National Renewable Energy Laboratory. (2023). 2030 National Charging Network: Examining U.S. fast-charging needs to support 2030 light-duty EV projections (NREL/TP-5400-85654). https: //docs.nrel.gov/docs/fy23osti/85654.pdf
[13] U.S. Department of Energy, Alternative Fuels Data Center. (2024). EVI-X toolbox. https: //afdc.energy.gov/evi-x-toolbox/